The Solvation of Cu^{2+} with Gas-Phase Clusters of Water and Ammonia

Bridgette J. Duncombe,† Khadar Duale, Annabelle Buchanan-Smith, and Anthony J. Stace*

Department of Physical Chemistry, School of Chemistry, The University of Nottingham, University Park, Nottingham NG7 2RD, United Kingdom

Received: March 2, 2007; In Final Form: April 24, 2007

A detailed study has been undertaken of the gas-phase chemistry of $[Cu(H_2O)_N]^{2+}$ and $[Cu(NH_3)_N]^{2+}$ complexes. Ion intensity distributions and fragmentation pathways (unimolecular and collision-induced) have been recorded for both complexes out as far as $N = 20$. Unimolecular fragmentation is dominated by Coulomb explosion (separation into two single charged units) on the part of the smaller ions, but switches to neutral molecule loss for $N > 7$. In contrast, collisional activation promotes extensive electron capture from the collision gas, with the appearance of particular singly charged fragment ions being sensitive to the size and composition of the precursor. The results show clear evidence of the unit $[Cu(X)_8]^{2+}$ being of special significance, and it is proposed that the hydrogen-bonded structure associated with this ion is responsible for stabilizing the dipositive charge on Cu^{2+} in aqueous solution.

Introduction

The wealth of recent publications on the static and dynamical behavior of Cu^{2+} in water and other solvents provides testament to the significance of this cation in both chemistry and biochemistry. Theory[1−5] and experiment[6−11] have sought to explore the immediate environment of the metal dication, and in particular to establish the configuration and coordination number of the first solvation shell. However, despite this high level of activity, there still remains considerable uncertainty as to the precise number of water molecules surrounding Cu(II) when in solution. The source of the problem is the Cu(II) d^9 electron configuration and the possibility that Jahn−Teller distortion will deform the regular octahedral solvent geometry routinely attributed to transition metal ions in aqueous solution.[12]

An alternative approach to the condensed phase is to examine the development of solvent structure surrounding metal cations in the gas phase.[13] A number of years ago, we produced the first mass spectrum confirming that stable $[Cu(H_2O)_N]^{2+}$ complexes could be generated in the gas phase.[14] Prior to that observation, there had been a suggestion that to stabilize the Cu^{2+} cation with water would require N to be at least 15 in order to suppress any tendency to undergo immediate charge transfer to give Cu^+.[15] The latter process being driven by the large difference (∼8 eV) in ionization energy between Cu^+ and water. Since that first experiment, several groups have shown that it is possible to generate and observe metastable $[Cu(H_2O)_N]^{2+}$ complexes down to $N = 1$,[16−18] and the gas-phase chemistry of Cu^{2+} has been studied in conjunction with a wide range of atomic and molecular species, many with ionization energies considerably lower than that of water.[19−23]

Possibly the most interesting result to emerge from those preliminary experiments on $[Cu(H_2O)_N]^{2+}$ complexes was the observation that the ion with the highest relative intensity contained eight water molecules.[14] A later experiment using ammonia also showed that $[Cu(NH_3)_8]^{2+}$ was at least a factor of 2 more intense than any of its nearest neighbors.[19] Both these observations were subsequently interpreted by Bérces et al.[24] using density functional theory, which showed that in the lowest energy configuration four water molecules coordinate directly to the metal cation in a structure, that because of Jahn−Teller distortion, is square-planar. A further four water molecules then occupy hydrogen-bonded sites whereby each additional molecule forms two hydrogen bonds with adjacent molecules on the square-planar ring. The stable arrangement of molecules obtained by Bérces et al.[24] is reproduced in Figure 1. For $[Cu(H_2O)_8]^{2+}$ this structure proved to be far more stable than if two of the molecules are assigned to axial sites on the central Cu^{2+} ion. For $[Cu(NH_3)_8]^{2+}$ differences in energy between a range of equatorial hydrogen-bonded structures and those that included molecules in axial positions, were calculated to be much smaller than for water.[24] Both theory[2,3] and experiment[9] would suggest that Jahn−Teller distortion has a significant destabilising influence on the development of solvent structure surrounding Cu^{2+}. The fact that $[Cu(NH_3)_8]^{2+}$ can adopt the structure shown in Figure 1 is particularly interesting because it means that those nitrogen atoms that participate in hydrogen bonding become five-coordinate. The appearance of a comparatively intense ion corresponding to $[Cu(H_2O)_8]^{2+}$ was subsequently verified by Stone and Vukomanovic.[25] These authors used electrospray, which is a significantly different approach to the pickup technique that had previously been used to generate the ion.

For both $[Cu(H_2O)_N]^{2+}$ and $[Cu(NH_3)_N]^{2+}$, the gas-phase experimental work presented thus far has been very preliminary. Apart from intensity distributions, there has been no additional experimental data presented to support the conclusion that units containing eight molecules are significantly different from their immediate neighbors. The purpose of this paper is to address that issue and present the results of a comprehensive experimental study of the physical and chemical behavior of $[Cu(H_2O)_N]^{2+}$ and $[Cu(NH_3)_N]^{2+}$ ions for $N \leq 20$.

* Corresponding author. E-mail: anthony.stace@nottingham.ac.uk.
† Present address: School of Chemistry, The University of Edinburgh, Joseph Black Building, The King's Buildings, West Mains Road, Edinburgh EH9 3JJ, U.K.

10.1021/jp0717286 CCC: $37.00
Published on Web 05/31/2007

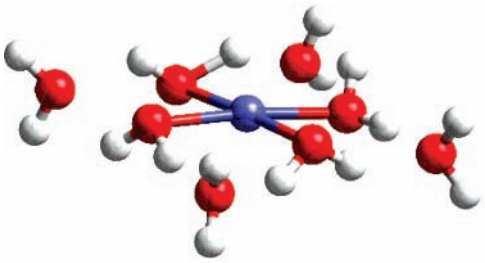

Figure 1. Structure proposed for $[Cu(H_2O)_8]^{2+}$, which has been adapted from the calculations of Bérces et al.[24]

Experimental Section

The experimental setup has been described in detail elsewhere.[26] Copper pieces were placed in an effusive source (DCA Instruments) and held at a temperature of 1230 °C, to yield $\sim 10^{-2}$ mbar of copper vapor. This region was crossed with a neutral beam of mixed ligand−argon clusters (L_NAr_M), which were formed by the adiabatic expansion of a vapor/argon mixture through a pulsed supersonic nozzle. For ammonia the vapor came from a mixed argon/ammonia cylinder containing 1% NH_3 and for water, argon was passed through a reservoir containing water held at a room temperature. The clusters passed through a 1 mm diameter skimmer into the path of the metal vapor, where the mixed solvent−argon clusters could pick up single copper atoms. Only rarely are metal dimers detected.[27] The neutral clusters then entered the ion source of a high-resolution double-focusing mass spectrometer (VG ZAB-E) where they were ionized by electron impact at 100 eV and extracted from the source with an acceleration voltage of 5 kV. In conjunction with the thermal pickup process, ionization is thought to cause complete evaporation of the rare gas atoms from the clusters (no ions of the form $[Cu(L)_NAr_M]^{2+}$ are detected, but $[CuAr_M]^{2+}$ complexes are seen if the expansion consists of pure argon).[28] Previous experiments have indicated that the presence of rare gas atoms is an essential part of the pick-up process.[29]

A shutter situated at the top of the oven provided an unambiguous assignment of signals due to metal-containing species, and values recorded for parent ion intensities represent differences between signals measured with the shutter open and closed. Such a procedure is necessary, as nonmetallic ligand clusters can dominate the total ion signal. Reaction products from both the unimolecular and collision-induced dissociation (CID) of size-selected complexes were identified by systematically scanning the voltage of the electrostatic analyzer;[30] a procedure that results in a mass-analyzed ion kinetic energy (MIKE) spectrum. For the purposes of promoting CID processes, the background pressure in a cell situated next to the single focusing slit in the second field free region of the mass spectrometer was increased to $\sim 10^{-6}$ mbar through the introduction of xenon.

This series of experiments has benefited from recent improvements in resolution and sensitivity that have been made to the mass spectrometer. Of particular significance to the results presented here is the ability to distinguish between electron capture processes, where a dication can acquire an electron from the collision gas, and Coulomb explosion, where a dication fragments into two singly charged units.[31] Previous studies have assumed fragmentation to be dominated by the latter. Ion intensity measurements were made using both ^{63}Cu and ^{65}Cu and presented as a weighted average. All other experiments involving size-selected complexes have been conducted using the ^{63}Cu isotope.

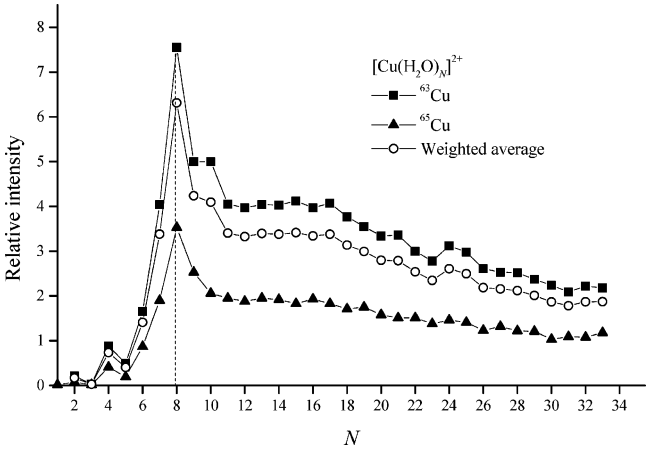

Figure 2. Distribution of relative intensities recorded for $[Cu(H_2O)_N]^{2+}$ ions as a function of *N*. Data are shown for ^{63}Cu and ^{65}Cu, together with a weighted average of the two separate measurements.

Results and Discussion

A. Signal Intensities and Fragmentation Patterns of $[Cu(H_2O)_N]^{2+}$ Complexes. Figure 2 shows an intensity distribution recorded for $[Cu(H_2O)_N]^{2+}$ complexes plotted as a function of *N*, where the shape confirms earlier measurements showing $[Cu(H_2O)_8]^{2+}$ as being a particularly intense combination of Cu^{2+} with water.[14] Also present in the earlier data was a local intensity maximum at $[Cu(H_2O)_4]^{2+}$ and this can also be seen in Figure 2, where the result is reproduced using both isotopes. In their calculations on $[Cu(H_2O)_N]^{2+}$ complexes, Bérces et al.[24] noted that the four-molecule water structure adopted a stable square-planar configuration; in contrast, their calculations on the corresponding ammonia complex showed the four-molecule structure to be nonplanar and, as a consequence, less stable. As will be shown below, there is no equivalent local maximum for $[Cu(NH_3)_4]^{2+}$ in the intensity data recorded for Cu^{2+}/ammonia clusters.

1. Unimolecular Decay. Measurements on size-selected $[Cu(H_2O)_N]^{2+}$ cations showed the unimolecular loss process

$$[Cu(H_2O)_N]^{2+} \rightarrow [Cu(H_2O)_{N-1}]^{2+} + H_2O \qquad (1)$$

to be present for $N > 6$. The base pressure in the flight tube of the mass spectrometer was maintained at approximately 5×10^{-8} mbar, and under these circumstances, the time scale for unimolecular decay (10^{-5}−10^{-4} s) of the ions is determined by residual energy remaining after electron impact ionization. It is assumed that fragmentation patterns recorded in this way can reveal stable structures that are independent of any perturbations that may occur during the preparation of complexes, for example, fluctuations in the gas mixing and expansion process or changes in the settings used for the ion source. The results of studying reaction 1 are shown in Figure 3 and display several interesting features. First, there is no evidence for unimolecular fragmentation below $N = 7$, and even for that ion the signal is extremely weak. Such behavior is unusual; many of the ion complexes studied previously have exhibited unimolecular decay down to $N = 3$ or 4, at which point charge transfer followed by Coulomb explosion begins to dominate.[31] However, Cu^{2+} does have the highest electron affinity of any of the metal dications found to be capable of forming stable complexes with water. Previous experiments with Ag^{2+}, which has an even larger electron affinity,[26] failed to produce $[Ag(H_2O)_N]^{2+}$ ions. Confirmation of a switch in fragmentation pattern on the part of smaller $[Cu(H_2O)_N]^{2+}$ ions is given below where further

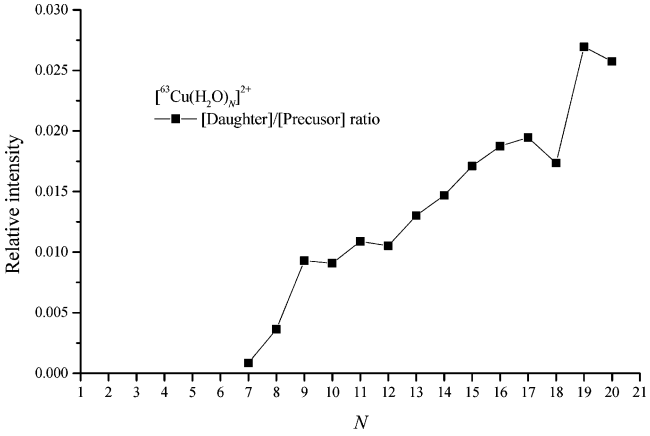

Figure 3. Relative intensity of the ionic fragment following the unimolecular loss of a neutral water molecule from each size-selected $[Cu(H_2O)_N]^{2+}$ ion. The measurements are plotted as a function of *N*.

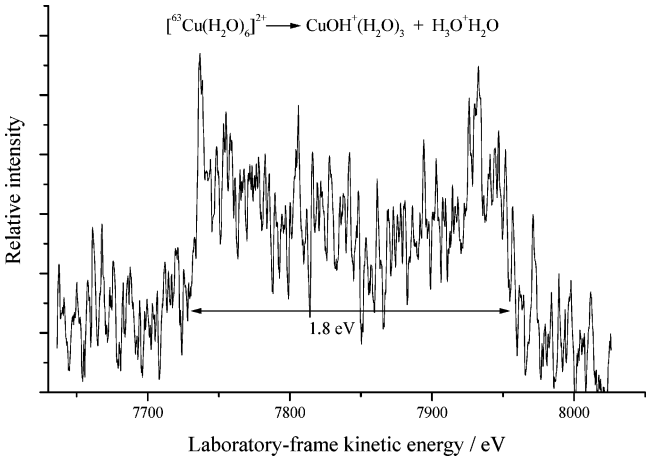

Figure 4. Kinetic energy profile recorded following the metastable unimolecular decay of $[^{63}Cu(H_2O)_6]^{2+}$ to produce $^{63}CuOH^+(H_2O)_3 + H_3O^+H_2O$. The peak shape is indicative of Coulomb explosion.

discussion on this topic is presented. Comparing the data for $N = 8$ and 9; the results show that $[Cu(H_2O)_9]^{2+}$ readily loses a water molecule, but that the comparatively more intense $[Cu(H_2O)_8]^{2+}$ ion is much less reactive (via reaction 1). This type of behavior has been used in the past to rationalize intensity data, such as that shown in Figure 2, in terms of the appearance of stable structures.[32] In this case, the intensity of $[Cu(H_2O)_8]^{2+}$ would increase at the expense of facile fragmentation by larger complexes and, at the same time, $[Cu(H_2O)_8]^{2+}$ would be reluctant to fragment further. However, the high intensity of $[Cu(H_2O)_8]^{2+}$ could also be accentuated by the instability of complexes containing fewer than eight molecules.

An alternative decay route open to multiply charged complexes is one where unimolecular fragmentation is accompanied by charge separation, and examples of such behavior have been reported earlier in experiments on $[Mg(NH_3)_N]^{2+}$.[31] In such cases, the ions are metastable with respect to crossing onto a repulsive potential energy curve that leads to Coulomb explosion. Since the latter step is more or less instantaneous, metastability on a time scale of $10^{-5} - 10^{-4}$ s is derived from a combination of the probability of curve crossing and the probability that sufficient energy will appear in a reaction coordinate that intersects with the Coulomb energy curve. Figure 4 shows an example of unimolecular charge separation (UCS) which involves $[Cu(H_2O)_6]^{2+}$ undergoing the processes

$$[Cu(H_2O)_6]^{2+} \rightarrow CuOH^+(H_2O)_3 + H_3O^+H_2O \qquad (2)$$

The peak has the characteristic dish-shaped profile associated with rapid decay accompanied by a substantial release of kinetic energy (~1.8 eV). Similar, but far weaker profiles were recorded for $N = 7$ and 8, with the latter being considerably less intense than the product arising from reaction (1). The observation of metastable Coulomb explosion on the part of ions as large as $[Cu(H_2O)_8]^{2+}$ is very unexpected; previous examples having been confined to complexes containing three or four solvent molecules.[31] However, the pattern does fit with the data given in Figure 3 and with the trend seen in earlier results for $[Mg(NH_3)_N]^{2+}$, which is that, as *N* decreases, Coulomb explosion takes over once neutral loss (reaction (1)) ceases to be observed.[31] A simple Coulomb potential calculation: R/Å = 14.4/T, using the kinetic energy release (*T*) values given above, shows an upper limit to the initial separation of the two positive charges in both $[Cu(H_2O)_6]^{2+}$ and $[Cu(H_2O)_8]^{2+}$ as 7.9 Å. Such a distance is slightly longer than would normally be attributed to the formation of a salt bridge between primary and secondary shell water molecules prior to fragmentation.[33] However, if some fraction of the Coulomb energy were to be dissipated into vibrational excitation of the reaction products, then charge separation could have been initiated at a distance shorter than 7.9 Å.

2. Collision- and Electron Capture-Induced Fragmentation. Additional studies of fragmentation in $[Cu(H_2O)_N]^{2+}$ have been conducted using collisional activation via the introduction of xenon ($\sim 10^{-6}$ mbar) into a gas cell located close to the focal point of the magnet in the second field-free-region of the sector mass spectrometer. In the interpretation of many earlier experiments it has been assumed that all charge reduction processes proceed via charge transfer and that any spread in laboratory-frame kinetic energy,[19,23] which is a signature of such reactions (see above), was due to Coulomb explosion. However, recent experiments conducted on $[Mg(NH_3)_N]^{2+}$ ions have highlighted the importance of electron capture as a charge reduction mechanism in dication complexes that undergo collisions at high relative velocities.[31] Coupled with improvements in instrumentation, these experiments have also revealed that many of the broad peaks seen in previous experiments are in fact composite, and that interaction with a collision gas can lead to one or both of the following electron capture dissociation (ECD) processes being observed:

$$[M(H_2O)_N]^{2+} + Xe \rightarrow M^+(H_2O)_{N-K} + KH_2O + Xe^+ \qquad (3)$$

$$[M(H_2O)_N]^{2+} + Xe \rightarrow MOH^+(H_2O)_{N-K-1} + KH_2O + H + Xe^+ \qquad (4)$$

M is a metal dication and *K* typically starts at 1, but can be zero under certain circumstances. As far as efficient electron transfer is concerned, signal intensities for electron capture from those gases examined have been found to follow the order Xe >> $N_2 \approx O_2$ >> He.[31] This trend correlates, more or less, with ease of ionization of the collision gas; however, it may be possible that polarization is also important if the difference in behavior between xenon and oxygen is to be explained. The cross-section for either of the above processes is sufficiently large that signals recorded at a background pressure of $\sim 10^{-7}$ mbar (of N_2) frequently include a residual contribution from electron capture. Depending on the value of *N* the above reactions were also found to be accompanied by contributions from collision-induced Coulomb explosion.

As an example of the variety of fragmentation processes observed in the $[Cu(H_2O)_N]^{2+}$ system, Figure 5 shows the result

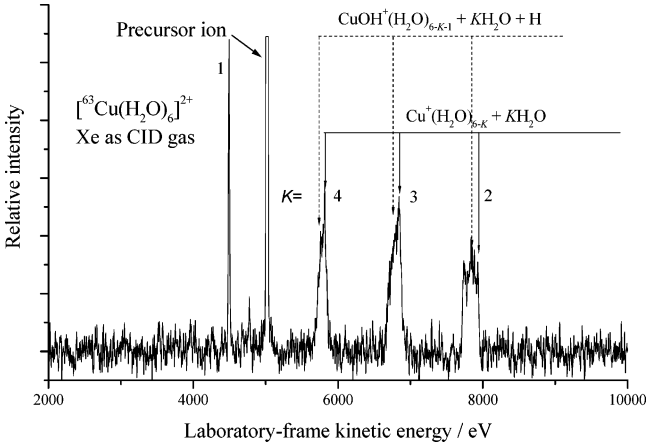

Figure 5. MIKE spectrum of $[^{63}Cu(H_2O)_6]^{2+}$ following collisional activation with xenon at a pressure of $\sim 10^{-6}$ mbar in the collision cell.

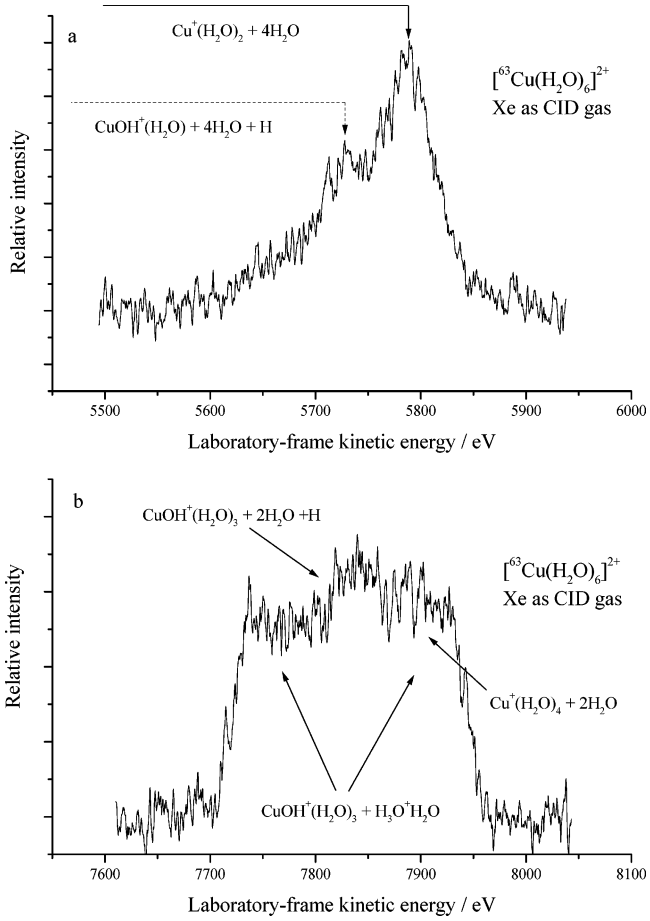

Figure 6. Expanded views of selected sections of Figure 5: (a) highlighting the products of electron capture; (b) the products of electron capture and Coulomb explosion.

of a MIKE scan undertaken on $[Cu(H_2O)_6]^{2+}$ in the presence of xenon as a collision gas. In addition to a single narrow peak due to reaction (1) there are three peaks that correspond to a variety of charge reduction processes. Expanded views of two of the peaks, which were recorded at a slower scan speed, are given in Figure 6. Figure 6a shows what is clearly a composite peak and the similarity in shape between individual peaks and those identified previously, leads us to believe that they are due to ECD in the form of

$$[Cu(H_2O)_6]^{2+} + Xe \rightarrow Cu^+(H_2O)_2 + 4H_2O + Xe^+ \quad (5)$$

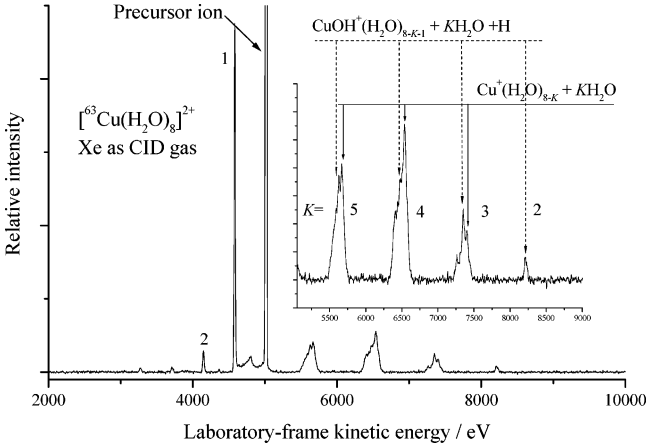

Figure 7. Same as for Figure 5, but for $[^{63}Cu(H_2O)_8]^{2+}$.

and

$$[Cu(H_2O)_6]^{2+} + Xe \rightarrow Cu^+OH(H_2O) + 4H_2O + H + Xe^+ \quad (6)$$

Compared with 6a, the peak profile shown in Figure 6b is quite different in shape, but is still believed to include contributions from the ECD steps

$$[Cu(H_2O)_6]^{2+} + Xe \rightarrow Cu^+(H_2O)_4 + 2H_2O + Xe^+ \quad (7)$$

and

$$[Cu(H_2O)_6]^{2+} + Xe \rightarrow Cu^+OH(H_2O)_3 + 2H_2O + H + Xe^+ \quad (8)$$

Removing the collision gas and repeating the scan (Figure 4 above) reveals an underlying dish-shaped peak that has already been attributed to metastable Coulomb explosion on the part of $[Cu(H_2O)_6]^{2+}$ undergoing reaction 2. Referring back to Figure 6b, the additional intensity compared with Figure 4, would suggest that the former also includes contributions from collision-induced as well as metastable Coulomb explosion.

Figure 7 shows a complete MIKE scan recorded following the collisional activation of $[Cu(H_2O)_8]^{2+}$, which exhibits many features in common with Figure 5, the scan for $[Cu(H_2O)_6]^{2+}$. An expansion of the $K = 3$ peak in Figure 7 shows components that can be resolved quite clearly into features attributable to reactions 3 and 4. Removal of the collision gas also reveals a very weak dish-shaped peak, which again can be assigned to metastable Coulomb explosion, with $[Cu(H_2O)_8]^{2+}$ undergoing charge separation to form $Cu^+OH(H_2O)_4 + H_3O^+(H_2O)_2$. However, when comparing Figures 5 and 7 in detail, a significant change in behavior can be seen: located at 8212 eV in Figure 7 is a peak showing $CuOH^+(H_2O)_5$ as the sole product of ECD, which contrasts with the composite peaks seen as fragments from $[Cu(H_2O)_6]^{2+}$ (and smaller complexes). A comparable fragment ion is also seen in the MIKE scan of $[Cu(H_2O)_7]^{2+}$ and corresponds to the appearance of $CuOH^+(H_2O)_4$ from reaction 4 with the complete absence of any contribution from reaction 3. This pattern of behavior marks a significant turning point in the distribution of product ions from ECD. Comparing the fragments $Cu^+(H_2O)_M$ and $CuOH^+(H_2O)_{M-1}$ from ECD, when M is ≤ 4 the dominant fragment is $Cu^+(H_2O)_M$ and when $M > 4$, the hydroxyl product is by far the more intense of the two product ions; in fact when M is >8, which is seen as a product for $N \geq 13$, the hydroxyl form is the only type of ion observed in the larger fragments. At the other extreme, the CID of $[Cu(H_2O)_2]^{2+}$ gives $Cu^+(H_2O)$ as the only fragment and the

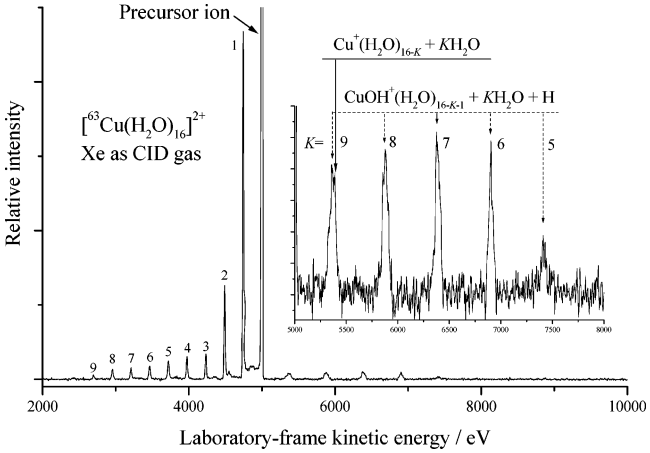

Figure 8. Same as for Figure 5, but for $[^{63}Cu(H_2O)_{16}]^{2+}$.

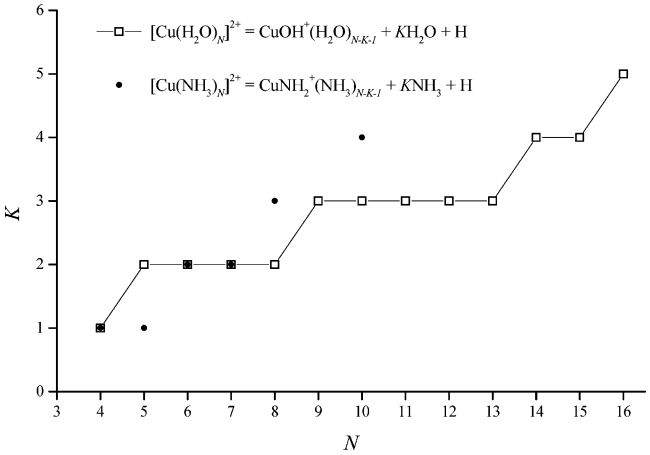

Figure 9. A plot of *K* against precursor complex size, *N*, where *K* is the minimum number of water molecules lost following the electron capture-induced dissociation (ECID) of each size-selected $[Cu(H_2O)_N]^{2+}$ and $[Cu(NH_3)_N]^{2+}$ complex.

very small spread in laboratory-frame kinetic energy present in the peak, would suggest that this ion is the product of ECD via reaction (3). Figure 8 shows a MIKE scan recorded for $[Cu(H_2O)_{16}]^{2+}$ and where the narrow ECD peaks can be seen switching from a predominantly hydroxyl product to a mixture of fragments emanating from a combination of reactions 3 and 4 as the value of *K* increases. What is also surprising about Figure 8 is that it shows electron capture continuing as a prominent charge reduction mechanism in clusters containing up to 16 water molecules (similar data of a slightly poorer quality has been recorded out as far as $N = 19$). In other examples studied thus far, ECD stops once *N* reaches 9 or 10 (see below).[31]

Related to the above discussion is an observation made on the value of *K* at which charge reduction begins in each of the MIKE scans on $[Cu(H_2O)_N]^{2+}$ complexes, for example in Figure 7, a peak corresponding to $K = 2$ can be seen. Figure 9 shows the lowest values observed for *K* plotted as a function of *N*. As can be seen, the data show distinct boundaries within which the complexes exhibit fixed patterns of behavior. Since the complementary product of ECD is neutral, it is assumed that the pattern seen in Figure 9 is influenced by: (i) the initial geometries of the precursor ions and (ii) the nature of the ionic product. Of particular relevance to the discussion surrounding $[Cu(H_2O)_8]^{2+}$ and the smaller cluster ions, is the fact that structures associated with the development of a second solvation shell all display the same critical size ($K = 2$) for the onset of a stable electron capture product. For the $K = 2$ series, the largest observed ECD fragment is $CuOH^+(H_2O)_5$, which could be seen as a stable primary-shell product emerging from a stable secondary-shell precursor. Figure 9 shows a further significant step ($K = 3$) with $[Cu(H_2O)_{13}]^{2+}$ becoming the next critical size of precursor ion; a possible structure for the latter might have the 2-D network shown in Figure 1, but extended through the addition of four further hydrogen-bonded water molecules and the final molecule then occupying one of the Jahn−Teller distorted axial sites. The fact that *K* remains fixed when associated with molecules in particular sites suggests that a limited amount of excess energy is available to promote dissociation following electron capture.

There are several aspects to the results presented here for $[Cu(H_2O)_N]^{2+}$ complexes that warrant further discussion. First, there are differences between the fragmentation patterns seen here and those given previously by Stone and Vukomanovic in their study of the dissociation of $[Cu(H_2O)_N]^{2+}$ complexes at low collision energies.[25] These authors observed only $CuOH^+(H_2O)_M$ fragments as opposed to the latter plus $Cu^+(H_2O)_M$ seen here. In addition, Stone and Vukomanovic also observed the complementary $H^+(H_2O)_P$ ions up to $P = 4$.[25] Absence of the latter in our experiments is not unexpected; first, these fragment ions are comparatively light and so could be lost through instrumental discrimination, and second they are not a product of electron capture and the reaction steps that do generate them, e.g., reaction 2, give very weak signals. For the most part, the different patterns of behavior can be explained by the energy dependence of the electron capture cross-section; for an increase in center of mass collision energy of 2 orders of magnitude, an electron capture cross section can also increase by ~100.[34] Since electron capture cross-sections are very much larger than those for collisional activation, the former process results in far less scattering of ions. Therefore, instrumental discrimination, which has a significant influence on our ability to detect fragment ions, is kept to a minimum.

What is less clear is why electron capture yields both $CuOH^+(H_2O)_M$ and $Cu^+(H_2O)_M$ fragments? Part of the answer to this question may lie in the relative binding energies of the hydroxyl group and water to Cu^+. In their study of CID pathways in $CuOH^+(H_2O)_{1,2}$ ions, Vukomanovic and Stone concluded that the Cu^+-OH bond was weaker than that of Cu^+-OH_2 when in the presence of both one and two water molecules.[25] Support for this result comes from calculations by Trachtman et al.[35,36] who give the bond enthalpies of Cu^+-OH and Cu^+-OH_2 as 118 and 158 kJ mol^{-1}, respectively. The latter value is also supported by experimental measurements; but unfortunately, no comparable experimental data are available for Cu^+-OH.[37] Our results show a gradual decline in the relative intensities of $CuOH^+(H_2O)_M$ fragments as *M* becomes smaller, with a critical fragment size that appears to be in the region of $Cu^+(H_2O)_5$ and $CuOH^+(H_2O)_4$ (~7400 eV in Figure 7): in smaller fragments, $Cu^+(H_2O)_M$ is the dominant electron capture product, but as Figure 8 shows, $CuOH^+(H_2O)_M$ is the only fragment once *M* becomes >8. This observation would suggest that the Cu^+-OH and Cu^+-OH_2 bond energies are comparable in $CuOH^+(H_2O)_4$; however, it is also possible that the Cu^+-OH unit gains stability through hydrogen bonding in the larger product ions.

B. Signal Intensities and Fragmentation Patterns of $[Cu(NH_3)_N]^{2+}$ Complexes. Figure 10 shows a plot of $[Cu(NH_3)_N]^{2+}$ ion intensity against *N*. Previous measurements were unable to resolve ions for odd values of *N*; however, that discrepancy has been rectified with these new experiments where the data

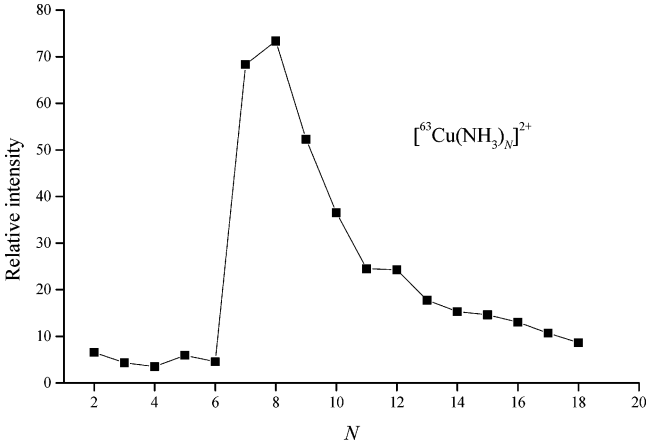

Figure 10. Distribution of relative intensities recorded for $[Cu(NH_3)_N]^{2+}$ ions as a function of *N*. The data points are weighted averages of separate measurements on ^{63}Cu and ^{65}Cu.

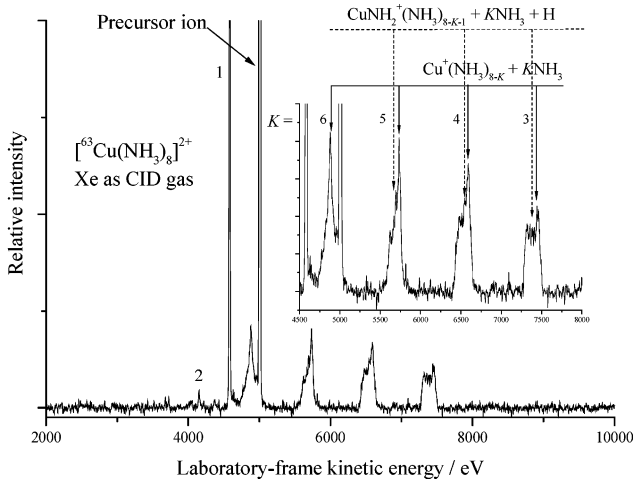

Figure 11. MIKE spectrum of $[^{63}Cu(NH_3)_8]^{2+}$ following collisional activation with xenon at a pressure of $\sim 10^{-6}$ mbar in the collision cell.

have confirmed the original conclusion that $[Cu(NH_3)_8]^{2+}$ is a particularly stable combination of Cu^{2+} with ammonia.[19] The differences in intensity between ion signals when *N* is less than 7 and $[Cu(NH_3)_8]^{2+}$ is far more pronounced than is seen for the corresponding water complexes, and unlike the water system there is no local maximum at $N = 4$. This latter observation is consistent with the calculations of Bérces et al.,[24] who found $[Cu(NH_3)_4]^{2+}$ to be slightly distorted away from a stable square-planar structure, which contrasts with the calculated results for $[Cu(H_2O)_4]^{2+}$. The very weak signals recorded for $[Cu(NH_3)_{N\leq 6}]^{2+}$ could, in part, be due to the lower ionization energy of ammonia (10.07 eV), which would serve to further destabilise any metastable complexes (see below).

The unimolecular fragmentation pattern recorded for $[Cu(NH_3)_N]^{2+}$ ions shows a pattern very similar to that seen for water in Figure 3. No loss of neutral NH_3 is observed once *N* is <7 and even at $N = 7$ that signal is extremely weak. However, there are small differences in behavior between the two systems and for comparison, Figure 11 shows a fragmentation pattern recorded following the collisional activation of $[Cu(NH_3)_8]^{2+}$. The appearance of stable fragments from ECD starts at $K = 3$ rather than 2 for water and contributions from the loss of just ligands (the equivalent of reaction 3, but for NH_3) rather than ligands + H (reaction 4) are more pronounced in ammonia than water. Both these observations are consistent with previous conclusions regarding the behavior of water. The greater loss of ammonia molecules compared with water from Cu^+ during ECD could be due to the former having slightly lower binding energies toward the metal ion in larger complexes,[24] and the reduced signals from the equivalent of reaction 4 could be due to the weaker hydrogen bond strength found for ammonia being less able to stabilize NH_2. At the other extreme, $[Cu(NH_3)_2]^{2+}$ shows evidence of forming both $CuNH_2^+$ and Cu^+NH_3 following collisional activation. Although the bond energies of $CuNH_2^+$ and Cu^+NH_3 follow the same pattern seen for water,[37] existing data show the energy difference between the two fragments to be much smaller and they may, therefore, be formed in competition. Further differences in ECD pattern are summarized in Figure 9, where it can be seen there is far less structure to the range of values observed for *K*. The broad peaks in Figure 11 denoting charge reduction are again composites that include, for example, contributions from the loss of $3NH_3$ and $3NH_3 + H$ as seen at a laboratory-frame kinetic energy of $\sim$7400 eV. Repeating the MIKE scan in this particular region, but without the collision gas, reveals a very weak dish-shaped profile due to metastable Coulomb explosion giving rise to $Cu^+NH_2(NH_3)_4 + NH_4^+(NH_3)_2$ as charge-transfer products. Again, it appears that a number of the composite peaks include contributions arising from three separate processes: unimolecular charge separation (UCS); collision-induced charge separation; and electron capture.

A further significant difference between water and ammonia comes from comparing the size of complex at which electron capture ceases to be an effective charge reduction mechanism. As noted earlier, complexes as large as $[Cu(H_2O)_{19}]^{2+}$ (and most probably beyond) continue to provide strong ECD signals, which contrasts with the $[Cu(NH_3)_N]^{2+}$ series, where any ECD signals have almost vanished by the time $N = 10$. We believe these differences may be due to the extent and structure of the hydrogen bond network emanating from the central ion, with the comparatively stronger bonds found for water leading to much larger and more stable planar configurations.

Conclusion

There is one result that dominates these experimental observations, which is that for these two hydrogen-bonded ligands, H_2O and NH_3, structures of the form $[Cu(X)_8]^{2+}$ appear to exhibit very distinctive properties. The initial interpretation, originating from the calculations of Bérces et al.,[24] was that $[Cu(X)_8]^{2+}$ represents a unique hydrogen-bonded structure that builds on the square-planar geometry that is characteristic of Cu(II) complexes. However, the new experimental data presented here have shown that the structure has (possibly!) a far more significant function, which is that it represents the minimum number of molecules required to transform $[Cu(X)_N]^{2+}$ complexes from being in a metastable state ($N < 8$) to a situation where the dication is in a stable solvent environment. The metastable states are characterized by an absence of reaction 1, which is replaced instead by a tendency for complexes to undergo Coulomb explosion. Since Coulomb explosion in this and other hydrogen-bonded systems always appears to be accompanied by proton transfer,[31] the formation of a structure, such as that shown in Figure 1, clearly facilitates that process. In examples where there are fewer ligands, Coulomb explosion has to be preceded by the promotion of a molecule from the first to the second solvation shell. As the value of *N* increases, the barrier to Coulomb explosion increases and eventually becomes greater than the barrier to the loss of a neutral molecule

(reaction 1). The critical size for that transition appears to be when $N = 8$. In effect, $[Cu(H_2O)_8]^{2+}$ could be considered as the unit that carries and stabilizes the double positive charge when Cu^{2+} is solvated in water.

There is a related issue associated with the ability of either water or ammonia to stabilize charge on Cu^{2+} and that is when comparisons are made with the behavior of Ag^{2+}. The difference in ionization energy between Cu^+ and ammonia (10.2 eV) is significantly larger than that between Ag^+ and water (8.8 eV); therefore, just on these values alone we might have expected to observe stable $[Ag(H_2O)_N]^{2+}$ ions.[26,38] Dications of both metals are more easily stabilized by nitrogen-containing ligands, which would favor the association of Cu^{2+} with ammonia. However, as shown earlier, ionic radius also makes an important contribution to stability (and metastability),[38] and the value for silver(II) at 79 pm appears to be sufficiently large as to cause significant overlap between the bound state and the repulsive Coulomb potential energy curve that leads to charge transfer. In contrast, the ionic radius of copper(II) at 57 pm is small enough to render even $[Cu(NH_3)_N]^{2+}$ stable.

There are distinct differences in behavior between $[Cu(NH_3)_N]^{2+}$ and $[Cu(H_2O)_N]^{2+}$, and these probably arise from how the respective hydrogen networks surrounding the cation develop as N increases. For $[Cu(H_2O)_N]^{2+}$ complexes to continue capturing electrons when N is ≥ 19 would suggest a very open structure, which allows an incoming xenon atom to gain access to the central Cu^{2+}. One possibility would be planar 2-D array of water molecules spreading out from the $[Cu(H_2O)_8]^{2+}$ core shown in Figure 1. In contrast, the 3-D nature of the ammonia molecule together with much smaller energy differences between the various 2- and 3-D options for $[Cu(NH_3)_8]^{2+}$, suggests a more closed structure that is able to suppress ECD once N becomes >10. This latter number would certainly be consistent with observations from other dication complexes that are assumed to adopt 3-D hydrogen-bonded structures.[31] Similarly, the lack of agreement between the water and ammonia data in Figure 9 would suggest differences in structure. The $[Cu(H_2O)_N]^{2+}$ data fit a pattern whereby excess energy from the ECD process removes successive shells of hydrogen-bonded molecules. The $N = 5-8$ shell being represented in Figure 1 and the $N = 9-13$ shell of water molecules being the next hydrogen-bonded layer. In contrast, the ammonia data reflect a variety of structures and, as N increases, the effects of a weaker hydrogen bond network than is seen for water become apparent.

The question then is what do these observations have to offer in terms of the coordination of Cu^{2+} in bulk water? The results clearly provide strong support for an underlying stable square-planar structure, which consists of a primary shell of four water molecules in an equatorial plane that, in turn, is held in place by a secondary lattice of four molecules occupying hydrogen-bonded sites. The overall eight-molecule structure acquires stability via the formation of charge-enhanced hydrogen bonds, which gain their strength from the primary shell water molecules being polarized by the 2+ charge on the central cation. Further evidence of this effect is to be seen in other structures calculated for hydrogen-bonded solvents in the presence of metal dications.[39] Calculations[24] and the experiments reported here suggest that the equivalent $[Cu(NH_3)_8]^{2+}$ unit is less stable than $[Cu(H_2O)_8]^{2+}$, and the electron capture data provide evidence that the 2-D lattice of water molecules propagating out from the central ion, maintains its integrity over a far wide range than is seen for ammonia.

The principal outcome of the calculations[24] and these experiments is that they clearly demonstrate just how destabilised the axial sites on $[Cu(H_2O)_8]^{2+}$ and $[Cu(NH_3)_8]^{2+}$ are as a result of Jahn−Teller distortion. A measure of that instability being the fact that the binding energy to an axial site must be less than that associated with hydrogen-bonded molecules in the secondary solvation shell. Given these circumstances, it is obvious why the rate of exchange of water molecules from axial sites on Cu^{2+} in bulk solution is very rapid[40] and that at any given instance, the number of water molecules in close proximity to the ion could easily be less than six.

Acknowledgment. The authors would like to thank EPSRC for financial support and for the award of a studentship to K.D.

References and Notes

(1) Curtiss, L.; Halley, J. W.; Wang, X. R. *Phys. Rev. Lett.* **1992**, *69*, 2435.
(2) Schwenk, C. F.; Rode, B. M. *J. Chem. Phys.* **2003**, *119*, 9523.
(3) Schwenk, C. F.; Rode, B. M. *Chem. Phys. Chem.* **2003**, *4*, 931.
(4) Burda, J. V.; Pavelka, M.; Šimánek, M. *J. Mol. Struct.* **2004**, *683*, 183.
(5) Amira, S.; Spångberg, D.; Hermansson, K. *Phys. Chem. Chem. Phys.* **2005**, *7*, 2874.
(6) Beagley, B.; Eriksson, A.; Lindgren, J.; Persson, I.; Pettersson, L. G. M.; Sandström, M.; Wahlgren, U.; White, E. W. *J. Phys.: Condens. Matter* **1989**, *1*, 2395.
(7) Persson, I.; Persson, P.; Sandström, M.; Ullström, A-S. *J. Chem. Soc., Dalton Trans.* **2002**, 1256.
(8) Benfatto, M.; D'Angelo, P.; Della Longa, S.; Pavel, N. V. *Phys. Rev. B* **2002**, *65*, 174205.
(9) Pasquarello, A.; Petri, I.; Salmon, P. S.; Parisel, O.; Car, R.; Tóth, E.; Powell, D. H.; Fischer, H. E.; Helm, L.; Merbach, A. E. *Science* **2001**, *291*, 856.
(10) Frank, P.; Benfatto, M.; Szilagy, R. K.; D'Angelo, P.; Della Longa, S.; Hodgson, K. O. *Inorg. Chem.* **2005**, *44*, 1922.
(11) Chaboy, J.; Muñoz-Páez, A.; Merkling, P. J.; Marcos, E. S. *J. Chem. Phys.* **2006**, *126*, 064509.
(12) Cotton, F. A.; Wilkinson, G. *Advanced Inorganic Chemistry*; Wiley: London, 1988.
(13) Stace, A. J. *J. Phys. Chem. A* **2002**, *106*, 7993.
(14) Stace, A. J.; Walker, N. R.; Firth, S. *J. Am. Chem. Soc.* **1997**, *119*, 10239.
(15) Blades, A. T.; Jayaweera, P.; Ikonomou, M. G.; Kebarle, P. *J. Chem. Phys.* **1990**, *92*, 5900.
(16) Schroder, D.; Schwarz, H.; Jainglin, W.; Wesdemiotis, C. *Chem. Phys. Lett.* **2001**, *343*, 258.
(17) Stone, J. A.; Vukomanovic, D. *Chem. Phys. Lett.* **2001**, *346*, 419.
(18) Shvartsburg, A. A.; Siu, K. W. M. *J. Am. Chem. Soc.* **2001**, *123*, 10071.
(19) Walker, N. R.; Firth, S.; Stace, A. J. *Chem. Phys. Lett.* **1998**, *292*, 125.
(20) Seto, C.; Stone, J. A. *Int. J. Mass Spectrom. Ion Process.* **1998**, *175*, 263.
(21) Seto, C.; Stone, J. A. *Int. J. Mass Spectrom.* **1999**, *192*, 289.
(22) Combariza, M. Y.; Vachet, R. W. *J. Phys. Chem. A* **2004**, *108*, 1757.
(23) Wright, R. R.; Walker, N. R.; Firth, S.; Stace, A. J. *J. Phys. Chem. A* **2001**, *105*, 54.
(24) Bérces, A.; Nukada, T.; Margl, P.; Ziegler, T. *J. Phys. Chem. A* **1999**, *103*, 9693.
(25) Stone, J. A.; Vukomanovic, D. *Int. J. Mass Spectrom.* **1999**, *185/186/187*, 227.
(26) Walker, N. R.; Wright, R. R.; Stace, A. J. *J. Am. Chem. Soc.* **1999**, *121*, 4837.
(27) Wu, G.; Stace, A. J. *Int. J. Mass Spectrom.* **2006**, *249/250*, 289.
(28) Walker, N. R.; Wright, R. R.; Barran, P. E.; Cox, H.; Stace, A. J. *J. Chem. Phys.* **2001**, *114*, 5562.
(29) Winkel, J. F.; Jones, A. B.; Woodward, C. A.; Kirkwood, D. A.; Stace, A. J. *J. Chem. Phys.* **1994**, *101*, 9436.
(30) Cooks, R. G.; Beynon, J. H.; Caprioli, R. M.; Lester, G. R. *Metastable Ions*; Elsevier: Amsterdam, 1973.
(31) Wu, B.; Duncombe, B. J.; Stace, A. J. *J. Phys. Chem. A* **2006**, *110*, 8423.
(32) Stace, A. J.; Moore, C. *Chem. Phys. Lett.* **1983**, *96*, 80.
(33) Beyer, M.; Williams, E. R.; Bondybey, V. E. *J. Am. Chem. Soc.* **1999**, *121*, 1565.
(34) Ishii, K.; Itoh, A.; Okuno, K. *Phys. Rev. A* **2004**, *70*, 042716.

(35) Trachtman, M.; Markham, G. D.; Glusker, J. P.; George, P.; Bock, C. W. *Inorg. Chem.* **1998**, *37*, 4421.
(36) Trachtman, M.; Markham, G. D.; Glusker, J. P.; George, P.; Bock, C. W. *Inorg. Chem.* **2001**, *40*, 4230.
(37) *Organometallic Ion Chemistry*; Freiser, B. S., Ed.; Kluwer: Dordrecht, The Netherlands, 1996; p 283.
(38) Walker, N. R.; Wright, R. R.; Barran, P. E.; Murrell, J. N.; Stace, A. J. *J. Am. Chem. Soc.* **2001**, *123*, 4223.
(39) Cox, H.; Wright, R. R.; Walker, N. R.; Stace, A. J. *J. Am. Chem. Soc.* **2003**, *125*, 233.
(40) Powell, D. H.; Helm, L.; Merbach, A. E. *J. Chem. Phys.* **1991**, *95*, 9258.